Science of the Total Environment 806 (2022) 150149

Contents lists available at ScienceDirect

Science of the Total Environment

journal homepage: www.elsevier.com/locate/scitotenv

Predicting intraurban airborne $PM_{1.0}$-trace elements in a port city: Land use regression by ordinary least squares and a machine learning algorithm

Joyce J.Y. Zhang [a], Liu Sun [a], Daniel Rainham [b], Trevor J.B. Dummer [c], Amanda J. Wheeler [d,e], Angelos Anastasopolos [a], Mark Gibson [f], Markey Johnson [a,*]

[a] Air Health Science Division, Health Canada, Ottawa, ON, Canada
[b] Healthy Populations Institute and the School of Health and Human Performance, Dalhousie University, Halifax, NS, Canada
[c] School of Population and Public Health, University of British Columbia, Vancouver, BC, , Canada
[d] Mary MacKillop Institute for Health Research, Australian Catholic University, Melbourne, VIC, Australia
[e] Menzies Institute for Medical Research, University of Tasmania, Hobart, TAS, Australia
[f] Division of Air Quality and Exposure Science, AirPhoton, Baltimore, MD, USA

HIGHLIGHTS

- LUR models developed for over 32 $PM_{1.0}$ trace elements and metals for 3 seasons.
- Novel shipping-related variables were important predictors for Ni and V models.
- OLS- & RF-LUR predicted high proportion of spatial variability for most elements.
- RF-LUR produced more accurate estimates and did not overpredict.
- Models are to be applied in epidemiological health studies.

GRAPHICAL ABSTRACT

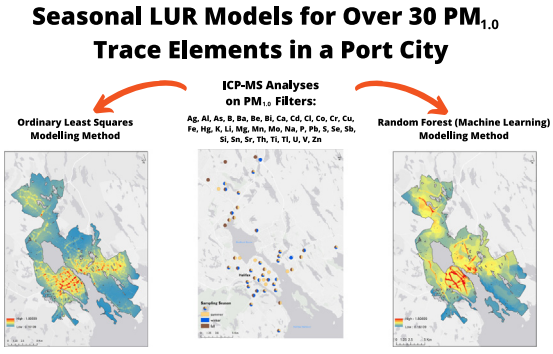

ARTICLE INFO

Article history:
Received 2 March 2021
Received in revised form 31 August 2021
Accepted 1 September 2021
Available online 6 September 2021

Editor: Philip K. Hopke

Keywords:
Outdoor air pollution
Pollution exposure
Land-use regression (LUR)
Particulate matter (PM)

ABSTRACT

Airborne particulate matter (PM) has been associated with cardiovascular and respiratory morbidity and mortality, and there is some evidence that spatially varying metals found in PM may contribute to adverse health effects. We developed spatially refined models for PM trace elements using ordinary least squares land use regression (OLS-LUR) and machine leaning random forest land-use regression (RF-LUR).

Two-week integrated measurements of $PM_{1.0}$ (median aerodiameter < 1.0 μm) were collected at 50 sampling sites during fall (2010), winter (2011), and summer (2011) in the Halifax Regional Municipality, Nova Scotia, Canada. $PM_{1.0}$ filters were analyzed for metals and trace elements using inductively coupled plasma-mass spectrometry. OLS- and RF-LUR models were developed for approximately 30 $PM_{1.0}$ trace elements in each season. Model predictors included industrial, commercial, and institutional/ government/ military land use, roadways, shipping, other transportation sources, and wind rose information.

RF generated more accurate models than OLS for most trace elements based on 5-fold cross validation. On average, summer models had the highest cross validation R^2 (OLS-LUR = 0.40, RF-LUR = 0.46), while fall had the lowest (OLS-LUR = 0.27, RF-LUR = 0.31). Many OLS-LUR models displayed overprediction in the final exposure surface. In contrast, RF-LUR models did not exhibit overpredictions. Taking overpredictions and cross validation

* Corresponding author at: Air Health Science Division, Health Canada, 269 Laurier Ave West, Ottawa, Ontario K1A 0K9, Canada.
E-mail address: markey.johnson@canada.ca (M. Johnson).

https://doi.org/10.1016/j.scitotenv.2021.150149

PM trace elements
Machine learning

performances into account, OLS-LUR performed better than RF-LUR in roughly 20% of the seasonal trace element models. RF-LUR models provided more interpretable predictors in most cases. Seasonal predictors varied, likely due to differences in seasonal distribution of trace elements related to source activity, and meteorology.

1. Introduction

Exposure to airborne particulate matter (PM) has been associated with cardiovascular and respiratory morbidity and mortality (Cohen et al., 2017; Hoek et al., 2013; Raaschou-Nielsen et al., 2013), and growing evidence suggests that metals may play a causal role in PM-related health impacts (Cakmak et al., 2014; Chen et al., 2020a, 2020b; Fang et al., 2017; Ostro et al., 2015). PM-related trace elements, including metals, display greater spatial heterogeneity compared with $PM_{2.5}$ mass (Jeong et al., 2011; Song et al., 2001). Therefore, spatially-resolved information is required to accurately assess exposure to PM-related metals in health studies.

Land-use regression (LUR) models have been widely used to characterize local-scale spatial variability in urban air pollution (Brauer et al., 2003; Hoek et al., 2008; Jerrett et al., 2007; Mukerjee et al., 2009; Ryan and Lemasters, 2007; Vienneau et al., 2010), and have been identified as the preferred method for estimating exposure to spatially heterogeneous pollutants (Health Effects Institute, 2010). LUR models have been used to estimate both gaseous pollutants (Bertazzon et al., 2015; Madsen et al., 2011; Su et al., 2010; Wheeler et al., 2008) and PM (Chen et al., 2010; Henderson et al., 2007; Rivera et al., 2012).

The LUR approach has also been applied to characterize the spatial distribution of trace elements associated with $PM_{2.5}$. De Hoogh et al. (2013) developed LUR models for eight elements associated with $PM_{2.5}$ in over fifteen European cities. LUR models have also been developed for $PM_{2.5}$ components in cities in the USA, Australia, and Taiwan (Brokamp et al., 2017; Dirgawati et al., 2016; Hsu et al., 2018; Ito et al., 2016; Li et al., 2016; Tripathy et al., 2019). We developed seasonal LUR models for $PM_{1.0}$ trace elements in Calgary, Alberta, Canada (Zhang et al., 2015), an inland city in the Canadian prairies with a large natural gas industry. However, few studies examine seasonal variations in spatial distributions and most explore only a limited number of elements.

The majority of LUR models have been developed using the ordinary least squares (OLS) method. Despite screening for variance inflation and variable heteroscedasticity, OLS-LUR models are prone to overprediction of ambient concentrations due to relatively small number of samples included in air pollution studies (Brokamp et al., 2017; De Hoogh et al., 2013). These challenges are more pronounced in LUR models for trace elements (Brokamp et al., 2017), whose concentrations can vary by orders of magnitude within an urban area. Machine learning has emerged as useful tools for addressing these issues and modelling the spatial distribution of urban air pollution (Brokamp et al., 2017; Chen et al., 2020; Chen et al., 2010; Liu et al., 2020; Requia et al., 2019; Weichenthal et al., 2016).

In particular, the random forest (RF) machine learning approach has performed well against traditional LUR modelling methods in comparison studies (Brokamp et al., 2017; Chen et al., 2019; Chen et al., 2020a, 2020b; Kerckhoffs et al., 2021; Liu et al., 2020; Ren et al., 2020). RF is an ensemble machine learning method that can overcome overfitting issues associated with a small number of samples and a large number of potential predictors (Breiman, 2001). This approach is particularly well-suited for examining the large number of collinear predictors considered for predicting spatial variation in trace elements. However, there has been a limited number of studies comparing OLS and RF modelling methods in the context of PM trace elements (Brokamp et al., 2017).

In this study, we developed the first spatially refined estimates of $PM_{1.0}$ metals and trace elements for a Canadian port city using simultaneous sampling of 33 $PM_{1.0}$ trace elements collected at 50 sites during 3 seasons. Our second objective was to assess and compare the strengths and limitations of OLS and RF approaches over a large set (80 pairs) of seasonal models. Lastly, we aimed to identify seasonal patterns of $PM_{1.0}$ trace elements in a port city using novel shipping, transportation, and meteorological predictors. This will support research to elucidate potential health impacts of air pollution, and the role of metals in mediating adverse health outcomes.

2. Methods

2.1. Study area

The Halifax Regional Municipality (HRM) is home to Eastern Canada's largest seaport. Seaport emissions (including ships and on-land equipment) are a major source of PM (Ault et al., 2009; Bailey and Solomon, 2004; Kuwayama et al., 2013; Lack et al., 2011) and have been associated with various health effects (Perez et al., 2009; Tian et al., 2013). HRM has relatively low levels of ambient air pollution compared to other Canadian cities (Environment and Climate Change Canada, 2018). However, as a result of shipping activities, the port area is characterized by higher pollution levels than the surrounding residential areas. Ambient concentrations of PM-elements associated with ship emissions, such as Ni and V (Agrawal et al., 2008; Celo and Dabek, 2011; Jeong et al., 2011; Lee and Hopke, 2006; Zhao et al., 2013), can be high compared with typical Canadian urban areas (Jeong et al., 2011).

HRM has a population of 390,328 (Statistics Canada, 2012) with 76% of the population living in the urban area within 6 km of the Halifax Harbour. HRM is characterized by various industrial and commercial emitters; marine shipping and related emissions in the port area; fishing service industries, mining, and forestry operations; as well as a wide range of institutional/ government/ military land use including 3 Canadian Armed Forces facilities and 6 post secondary institutions (DMTI Spatial, 2013; Government of Canada, 2018).

2.2. Sample collection and analysis

Air monitoring campaigns were conducted at 47 sites in fall (October 20–November 3, 2010), and winter (January 5–19, 2011), and at 53 sites in summer (August 11–25, 2011). Optimal sampling sites were identified using a location-allocation model based on land-use, transportation infrastructure and the distribution of at-risk populations (Kanaroglou et al., 2005). In addition, 10–12 sites were chosen using a combination of local knowledge and optimal spatial coverage to reduce the impacts of spatial autocorrelation. Two-week integrated $PM_{1.0}$ mass measurements were collected using Harvard Cascade impactors with 37 mm Teflon filters at a flow rate of 5 L/min. Thirty-six trace elements were analyzed from the $PM_{1.0}$ samples using inductively coupled plasma-mass spectrometry (ICP-MS). Trace elements are listed in section A1 of the online supplement.

Invalid data due to power loss or equipment malfunction were removed from the analysis. Pollutant data from 38 fall, 30 winter, and 36 summer sites were used in LUR analyses; 17 sites provided valid data in all three seasons, 37 sites provided valid data in at least two seasons, and 13 sites provided data in only one season (Fig. 1). Quality assurance, blank correction protocols, and definitions of detection limits (DL) are described in further detail in section A1 in the online supplement.

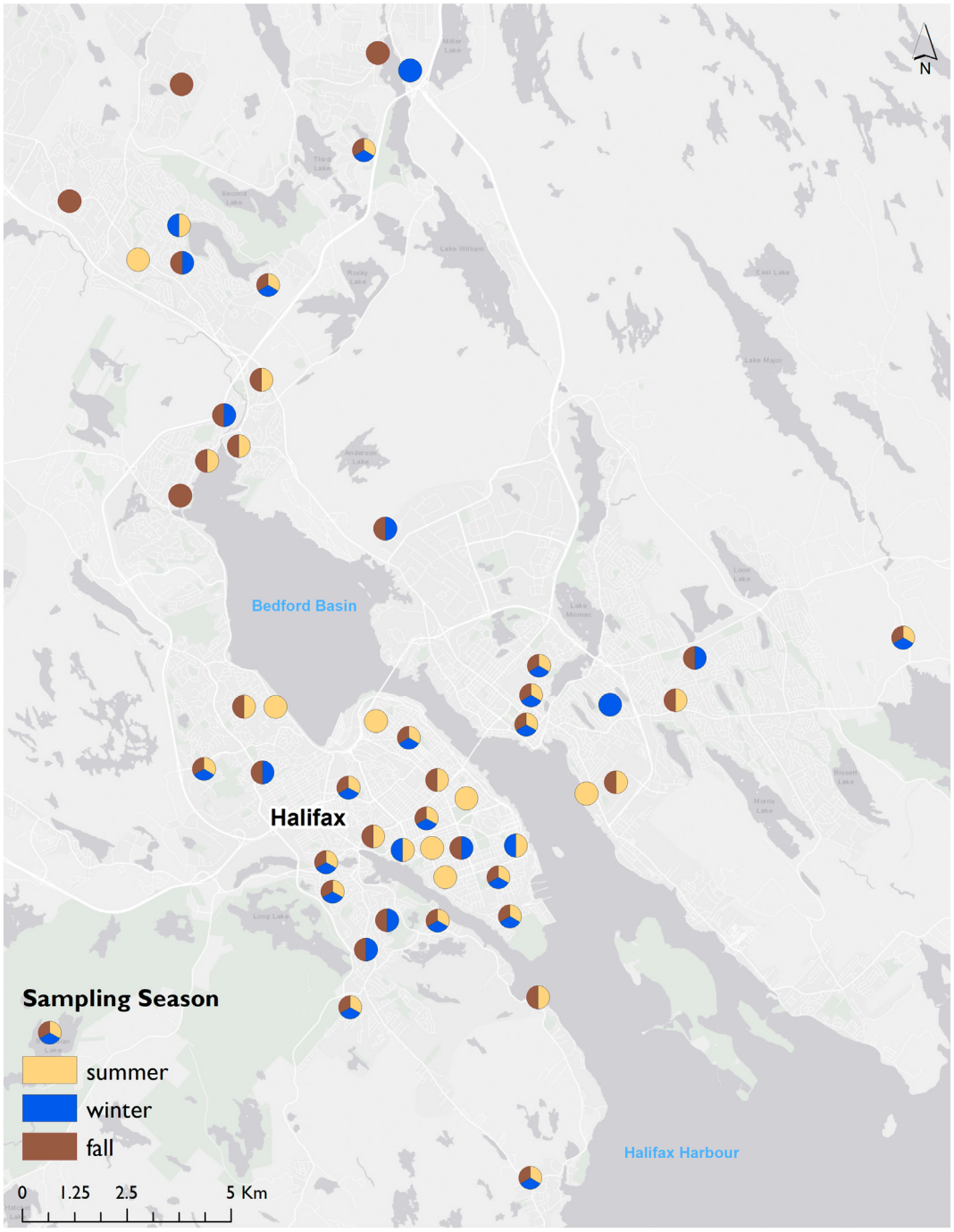

Fig. 1. Sampling sites used in seasonal LUR model development.

We conducted RF and OLS modelling for all elements with at least 50% of the seasonal measurements greater than DL—i.e., 31 trace elements in summer, 25 in fall and 29 in winter.

2.3. Land-use variables

We considered a broad suite of novel and traditional predictors. These predictors included industrial and commercial point sources, land transportation networks, population density, shipping, and land-use zoning. Point (e.g., industrial facilities) and line sources (e.g., road networks) were used to generate both buffer and distance to source variables, while area sources (e.g., zoning) were used to create buffer variables. Buffer sizes ranged from 50 m to 10 km except for industrial facilities, which ranged from 50 m to 30 km (see Table A in the online supplement for a full list).

Industrial facilities ($N = 55$ facilities) were obtained through Environment Canada's 2010 National Pollutant Release Inventory (NPRI). Subcategories were created for industrial facilities based on size (e.g., large, medium, and small emitters) and type of emissions (e.g., $PM_{2.5}$ emitters, metal emitters, possible metal emitters). Facilities that were possible metal emitters were identified based on their North American Industry Classification System (NAICS) code combined with emissions characterizations for those industries reported in the literature (Environment Canada and Health Canada, 1993; Environment Canada and Health Canada, 1994a; Environment Canada and Health Canada, 1994b; Environment Canada and Health Canada, 1994c; Environment Canada and Health Canada, 2001; European Commission,

2000; Fishbein, 1981; Lockeretz, 1974), as described in Zhang et al. (2015).

Land-use zoning information was also obtained from Desktop Mapping Technologies Incorporated 2013.2a (DMTI) (DMTI, 2013). Land-use categories included industrial, commercial, institutional/ government, residential, parks/ open space, and ocean. Novel land-use information about military, fish or farming industry, ferry, coast, and shipyard/ wharf land-use, were obtained from the STAR survey (Millward and Spinney, 2011).

Commercial facilities data were obtained from DMTI. Novel commercial source predictors were generated for gas stations; industrial and commercial machine shops; and primary metal industries; as well as welding repair; stone products, ceramic and clay, glass products, and concrete and brick; and wood and lumber product facilities.

Road network data containing expressways, primary highways, major roads, and local roads were obtained from DMTI. Novel transportation predictors relating to railroads, truck routes, bus routes, bus stops, and road junctions were developed using information obtained from the Halifax regional Space Time Activity Research (STAR) survey (Millward and Spinney, 2011).

Population counts at the dissemination block (DB) level were obtained from Halifax Census data (Statistics Canada, 2008). Population density within each buffer was calculated by taking the sum of population counts from relevant DBs based on the proportion and divided by the buffer area.

Predictor variables were calculated as distance variables, circular buffer variables, and wind rose buffer variables. Distance variables, e.g., distance to the nearest point source or distance to the nearest major roadway, were determined as the Euclidean distance between each sampling site and the attribute of interest (i.e. the nearest industrial facility or major roadway). Circular buffer variables were calculated using the quantity of the attribute of interest (i.e. the number of points of interest or facilities, sum of road segment lengths, or total area of a zoning type within the circular buffer), divided by the area of the circular buffer. In addition to traditional circular buffers, wind rose buffers were created to capture the impact of seasonal wind directions and wind speeds on pollutant dispersion from potential sources. Both circular and wind rose variables are described in further detail by Zhang et al. (2015). Section A2 in the online supplement further describes the wind speeds and directions for the three seasons. A total of 1572 potential predictor variables were created for each season. A full list of potential predictors is provided in Table A in the online supplement.

In order to facilitate clear presentation of our results and discussion, subcategories of model predictors were grouped under the following source categories:

Road Networks: expressways, highways, major and minor roads, and truck routes.
Other Traffic Indicators: bus routes, bus stops, and road junctions.
Railroads: railroad land-use.
Industrial: industrial point sources and industrial land-use.
Commercial: commercial point sources, commercial and fish/farm industry services land-use.
Institutional/Government/Military: institutional & government, and military land-use.
Marine Related: shipyard or wharf land-use, areas of ocean, distance to coast, and distance to ferry port.
Population/Residential: population density and residential land-use.
Parks/Open Space: park and open space land-use.

2.4. OLS-LUR model development

From an initial pool of 1572 variables, we initially screened out potential predictors without discernible spatial variation in the study area. Then we compared highly correlated (Pearson correlation ≥0.60) variables within the same subcategory, and retained those with smaller buffer sizes because smaller buffers may be able to capture more localized spatial variation in the final model surfaces. This screening narrowed the pool of potential predictors to less than 200 (179 to 195 variables depending on the season). The next phase of screening compared the remaining variables across subcategories to trace element concentrations. For each pair of correlated potential predictors, the variable that was less correlated with the trace element of interest was eliminated. The correlation threshold used to identify highly correlated predictors across subcategories varied to arrive at a unique set of 30 potential predictors for each $PM_{1.0}$ trace element per season to ensure a reasonable computational time for the OLS regression model development.

We followed the methods used in Zhang et al. (2015) for OLS regression model development. Using the all subsets regression method, models with all possible combinations of 3 to 6 predictors (i.e., $\sum_{i=3}^{6} C(30, i) = 498\,771$ models per element season) were generated with the log-transformed (base e) trace element concentration as the dependent variable and a corresponding unique set of 30 predictors as the independent variables. Models with poor interpretability (e.g., source variables inversely associated with pollutant concentrations) were eliminated. We then assigned three rankings to each model for goodness of fit based on the adjusted coefficient of determination (adj-R^2), Akaike information criterion (AIC), and Mallows' CP (CP). An overall ranking for each model was calculated as the average of the three goodness of fit rankings. We then selected the top 200 ranked models and eliminated those with highly collinear variables (i.e., maximum variance inflation factor (VIF > 5)), and poor model residuals (i.e., 1.6 ≥ Durbin-Watson statistic ≥ 2.4, Shapiro-Wilk statistic ≤ 0.05, Cramér–von Mises criterion ≤ 0.05, Anderson–Darling statistic ≤ 0.05, and Pearson's chi-squared statistic ≤ 0.05). We used the Global Moran's I to evaluate the spatial autocorrelation of residuals in the top-ranked model(s), and eliminated models with spatial autocorrelation. The remaining top-ranked model was chosen as the final OLS-LUR model.

2.5. RF-LUR model development

We followed the general procedure described in Genuer et al. (2010) for finding a small number of variables sufficient for a good prediction of the dependent variable. With an initial pool of 1572 potential predictors and log-transformed (base e) trace element concentrations as the dependent variables, the mean and standard deviation of variable importance (VI) was calculated for each variable after 50 random forest runs (ntree = 2000, mtry = default for regression); then ranked from highest to lowest mean VI. Next, the mean of the VI standard deviations was used as a threshold for variable elimination—variables with a VI standard deviation higher than the threshold were retained since higher standard deviations indicate true variables (Genuer et al., 2010). Then a sequential variable introduction was used to create the final RF-LUR starting with the highest ranked variable (based on mean VI). Only variables that significantly decreased the out-of-bag (OOB) error of the model were retained as per Genuer et al. (2010). Final model surfaces, pseudo-R^2 $\left(\frac{1-mse}{Var(y)}\right)$ (Liaw and Wiener, 2001), and predictor importance were calculated as an average of five random forest runs. The spatial autocorrelation of residuals was also assessed on the final model.

2.6. Cross validation and model evaluation

We used 5-fold cross validation (CV) to assess model accuracy and compare OLS- and RF-LUR models. Sample points were randomly divided into five groups—one group was held out as the test group while the remaining four groups were used to train a model with the final OLS-LUR and RF-LUR variables. Groups were rotated to allow each group a chance to be the test group. The mean and standard deviation ($n = 5$) of the root mean squared error (RMSE) was calculated, as

well as the out-of-fold (OOF) RMSE, which is the RMSE calculated by combining all five test groups. We also plotted the OOF predicted concentrations against the sampled (measured) concentrations and compared the R^2 (CV R^2) and slope (CV slope) of the best-fit line. The difference in CV results were not significant when they are within 10% of the OLS-LUR values.

Model overprediction compared to the measured data was defined as follows:

- Large area with elevated concentrations - greater than 5% of the study area with an estimated concentration greater than the mean sampling concentration plus 3 standard deviations; or
- Unrealistic maximum concentration - the maximum estimated concentration was greater than 5 times the maximum sampled concentration (i.e. $\frac{Estimated\ Max}{Measured\ Max} > 5$).

2.7. Statistical and spatial analyses

ArcMap 10.3 (ESRI 2004 and 2012) was used to generate 1572 potential predictors; as well as creating the final OLS-LUR 20 m by 20 m model surfaces, and visualization of the RF-LUR model surface. WindRose PRO3 (Enviroware srl, 2016) was used to generate wind rose-shaped buffers based on wind directions and speeds measured at the Environment Canada weather station at Stanfield International Airport in HRM for each sampling period (online supplement fig. A).

SAS 9.4 (SAS, 2013) was used for OLS-LUR variable selection, model development and model evaluations. SAS 9.2 (SAS, 2008) was used for ANOVA analyses to assess seasonal concentration differences. Spatial autocorrelation for OLS-LUR and RF-LUR models was evaluated in R 3.4 (R-Project, 2017), using packages spdep (Bivand and Wong, 2018) and ape (Paradis and Ape, 2019), respectively. The R randomForest package (Liaw and Wiener, 2001) was used to generate RF-LUR models and the final 5 m by 5 m exposure surfaces. Five-fold cross validation of OLS- and RF-LUR was conducted using R 3.4. ArcMap (ESRI 2004 and 2012) was used to generate all map figures. Microsoft Excel, 2016 (Microsoft, 2016) was used to create all other figures.

3. Results

3.1. Sampled $PM_{1.0}$-elemental concentrations

Descriptive statistics for seasonal sampling results are provided in Table B in the online supplement. There were significant differences in seasonal concentrations for most of the $PM_{1.0}$ elements. Trace element concentrations were mostly higher in summer or winter versus fall. Trace elements with the highest degree of spatial variability were Cu, Mn, and Th, which had coefficients of variation (CoV) ≥ 90% across all three seasons. Na, Se, and Tl showed the least spatial variability, with CoV ≤ 20% in all three seasons. Spatial variability for most elements was highest in winter or fall.

3.2. Model performances

3.2.1. Model R^2s

OLS- and RF-LUR model pairs were developed for $PM_{1.0}$ trace elements in summer ($N = 30$), fall ($N = 23$) and winter ($N = 27$). Examples of OLS- and RF-LUR surfaces are shown for Ba and Ni in Figs. 3 and 4, respectively. In addition, six RF-LUR models were developed (summer Pb; fall Ca, Mg and Tl; winter As and Sr) for which the OLS-LUR method was unable to identify a final model. Our results focus on the 80 matched pairs of OLS- and RF-LUR models. In general, both OLS- and RF-LUR models performed better in summer and winter, compared to fall. Tables C—H in the online supplement show model R^2s and pseudo-R^2s, along with model predictors listed in order from the highest partial-R^2 or VI to the lowest for all seasonal models. Pseudo-R^2 values for RF-LUR models are not directly comparable to R^2 values for OLS-LUR models; however, they showed a moderate relationship (Pearson correlation = 0.52). Spatial autocorrelation of OLS- and RF-LUR residuals was minimal ranging between −0.29 to 0.35 and − 0.18 to 0.13, respectively.

3.2.2. Model cross validation

Five-fold cross validation results showed RF-LUR had higher precision and accuracy compared to OLS-LUR for most trace elements. Fig. 2a-c shows OOF CV R^2 and CV slope deviance from the perfect CV slope of 1 (i.e., 1 – CV slope) for OLS- and RF-LUR models (mean RMSE and OOF RMSE values are listed in tables C—H of the online supplements alongside final model predictors). A greater number of RF-LUR models outperform their OLS-LUR counterpart in all CV performance metrics, with the exception of fall OOF RMSE. Model CV performance for individual elements varied across seasons, and no trace element consistently achieved higher precision and/or accuracy across all seasons when modelled strictly by RF-LUR or OLS-LUR.

The mean CV R^2 was 0.34 and 0.39 for all OLS-LUR and RF-LUR, respectively. Seasonally, summer models exhibited the highest CV R^2 (OLS-LUR = 0.40, RF-LUR = 0.46) while fall models had the lowest (OLS-LUR = 0.27, RF-LUR = 0.31). A few trace-elements (summer Ni and V; winter Co) showed high CV R^2s (≥ 0.70) for both RF-LUR and OLS-LUR models, but the majority of trace elements had lower CV R^2s (≤ 0.50) for both model types. Similarly, CV slope deviance showed better performance from RF-LUR (0.61) compared to OLS-LUR (0.65). Seasonally, summer had the lowest deviance (OLS-LUR = 0.60, RF-LUR = 0.54) and fall had the highest (OLS-LUR = 0.73, RF-LUR = 0.69).

3.2.3. Model overpredictions

Over one-third of the final OLS-LUR maps displayed overprediction (47% in summer, 41% in fall, and 37% in winter). There were no consistent spatial patterns or specific locations that were more prone to OLS-LUR overprediction. Overpredictions were not associated with the skewness or kurtosis of the measured or log-transformed concentrations. Many overpredicted surfaces exhibit large areas with elevated concentrations and an unrealistic maximum concentration. In some cases, model surfaces had maximum concentrations that were greater than 100 times the maximum sampling concentration: summer Ag, Al, Mn, P, Sb, and Ti; winter Sb, Si, Sn, Th, and Ti; fall Ag, B, Ni, P, and Sn. Examples of overpredicted surfaces are shown in Figs. 3a (Ba) and 4a (Ni).

In marked contrast, RF-LUR models did not exhibit overpredictions compared with the measured data (see Figs. 3b (Ba) and 4b (Ni) for example). All RF-LUR estimates were within the range of measured seasonal minimum and maximum concentrations. In most cases RF-LUR models present were biased low for the highest observations and high for the lowest observations, which echoes findings reported by Reid et al. (Reid et al., 2015).

3.3. Model predictors

The most common model predictor categories showed variability by season. In summer and winter models, for both OLS- and RF-LUR methods, commercial, road networks and industrial predictors were most common. For fall models, the most common categories in OLS-LUR models were road networks, commercial, and a tie between industrial and institutional predictors; in RF-LUR models they were road networks, commercial, and industrial. We observed seasonal differences in final OLS- and RF-LUR model predictors for most trace elements. In general, RF-LUR models incorporated a larger number of predictors than OLS-LUR models; however, OLS-LUR included a more diverse set of predictors from different categories.

The summer sampling period was characterized by relatively consistent prevailing wind direction and speeds. Winter wind direction showed greater variability, but wind speeds were relatively stable. As the transition season between summer and winter, fall wind directions

oscillated between the prevailing wind directions characteristic of summer (southwest) and winter (northwest). The contribution of wind rose variables varied seasonally. Wind rose variables contributed to almost all RF-LUR models (summer: 97%, fall: 96%, winter: 89%) while contributions for OLS-LUR models varied by season (summer: 97%, fall: 59%, and winter 56%).

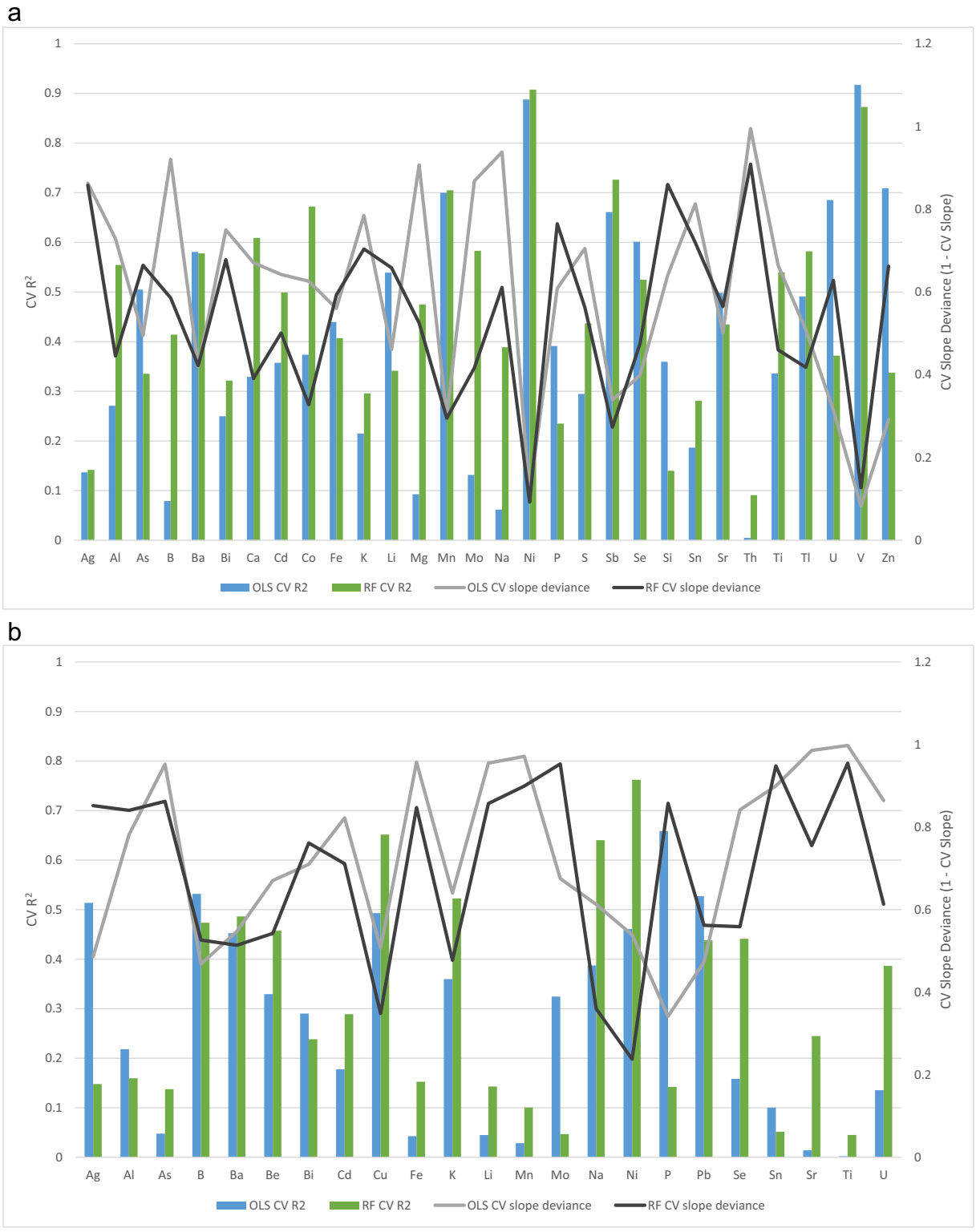

Fig. 2. a: Summer CV R^2 and CV slope deviance (the difference from the perfect slope of 1) results. The CV line of best fit was calculated using the out-of-fold predicted concentrations vs. the observed concentrations.
b: Fall CV R^2 and CV slope deviance (the difference from the perfect slope of 1) results. The CV line of best fit was calculated using the out-of-fold predicted concentrations vs. the observed concentrations.c: Winter CV R^2 and CV slope deviance (the difference from the perfect slope of 1) results. The CV line of best fit was calculated using the out-of-fold predicted concentrations vs. the observed concentrations.

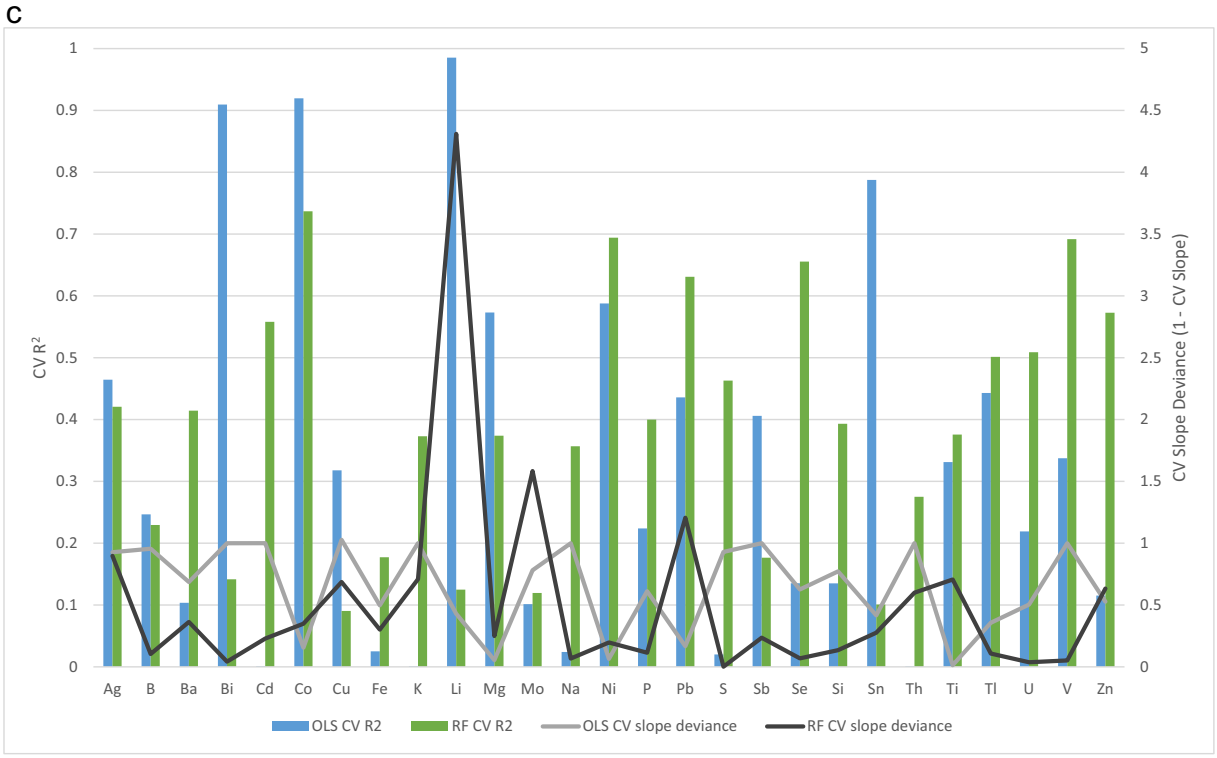

Fig. 2 (*continued*).

4. Discussion

We developed seasonal models for $PM_{1.0}$ trace elements based on fall, summer and winter air monitoring in the Halifax Regional Municipality, Nova Scotia, Canada. The study compared traditional (OLS) and machine learning (RF) approaches for developing spatially refined models. We also examined an extensive suite of predictors including a variety of novel port-related sources, commercial and transportation predictors, and wind rose predictors to incorporate meteorological information.

4.1. Intraurban airborne trace element concentrations

Distributions of measured $PM_{1.0}$ trace elements differed significantly between seasons. Trace element concentrations were typically higher in summer or winter, and most trace elements displayed greater spatial variability in winter or fall. Elevated concentrations for some elements in winter may have been due to winter fuel consumption patterns (Statistics Canada, 2017), as well as weather conditions favourable for particle buildup (i.e., reduced mixing height) (Masiol et al., 2020).

Some trace elements exhibited a higher degree of spatial variability (e.g., Ba, Cu, K, Mn, Ni, Th), suggesting substantial contributions from local sources. Others showed minimal spatial variability(e.g., Na, Se, and Tl), suggesting dominant contributions from regional sources via long-range transport. These results are consistent with Na being associated with marine aerosols and Se being associated with coal-fired power generation in the northeast United States (Gibson et al., 2013; Jeong et al., 2011).

4.2. OLS-LUR and RF-LUR model performance

OLS- and RF-LUR models explained a good portion of the spatial variability of most $PM_{1.0}$ trace elements across three seasons. In most cases, the RF pseudo-R^2 was lower than the OLS R^2 by 0.05 to 0.30, which is consistent with Brokamp et al. (2017). However, even with the very extensive suite of predictors we considered it was not adequate for predicting some trace elements, raising the question of whether these elements can be modelled accurately using LUR models alone.

OLS-LUR models significantly overpredicted ambient concentrations for many trace elements. Overpredictions were not related to the highly skewed distributions of many trace elements or poor CV results. This suggests non-linear relationships may exist between land-use predictors and concentrations. OLS-LUR overprediction is not novel to this study and has been documented in Brokamp et al. (2017) and Chen et al. (2020a, 2020b). Brokamp et al. (2017) developed RF models to address overpredictions at their sampling sites, which is the same approach as this study. Chen et al. (2020a, 2020b) truncated overpredicted values, which can result in a loss of spatial distribution gradient/information resulting in areas with no variation, especially when overprediction occurs to large regions.

RF-LUR models developed in this study had lower pseudo-R^2 than the RF-LUR models developed for 11 $PM_{2.5}$ related metals in Cincinnati, OH (Brokamp et al., 2017). The differences in RF-LUR performances may be due to differences in location, the PM size fraction ($PM_{2.5}$ vs. $PM_{1.0}$), or the highly skewed concentration distributions found in HRM compared with the Cincinnati study.

This study compared OLS and RF methods across 80 pairs of models, far exceeding the number of comparisons in many recent studies (Brokamp et al., 2017; Chen et al., 2019). As shown in Fig. 2, RF-LUR out-performed OLS-LUR in the majority of model pairs in every CV metric (mean RMSE, OOF RMSE, CV R^2 and CV slope), consistent with other studies' findings. However, each CV metric had 12–44% of model pairs with better OLS performance (5–18% after excluding overprediction models), and 12–21% of model pairs with not significant differences (< 10%) between the two methods. For model pairs with not significant differences, the simpler and more direct method (OLS) could be preferred because the more complex method (RF) did not yield significant improvement in prediction accuracy and precision (Weichenthal et al., 2016). Including pairs in which OLS models performed similarly or better compared to RF, OLS was the optimal LUR method for 20–30% of the seasonal trace element models, which is consistent with the results of

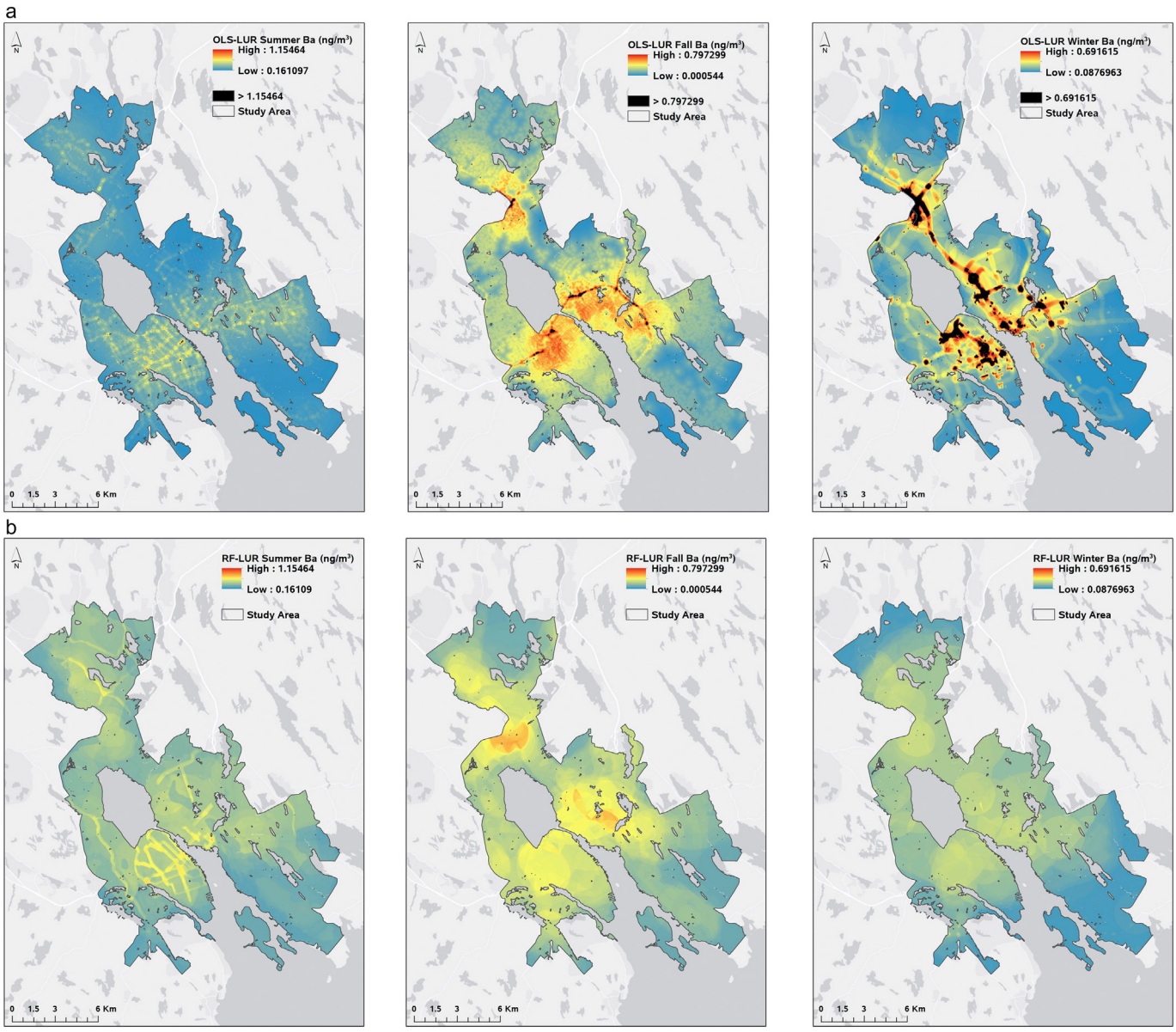

Fig. 3. a: Ba OLS-LUR exposure surfaces in three seasons (left to right: summer, fall, winter). The black areas indicate estimates higher than the maximum measured concentration for that season (not overprediction). Overprediction occurs in the winter surface where the maximum predicted concentration is 8.80 ng/m^3.
b: Ba RF-LUR exposure surfaces in three seasons (left to right: summer, fall, winter). The maximum on the colour scale aligns with the maximum observed concentration for that season.

Brokamp et al. (2017). Thus, from a model performance perspective, RF produced more accurate models for trace air pollution elements. The traditional OLS-LUR can be a viable complementary model because they are simpler and can be, in some cases, equally or more accurate. However, further research in different geographic locations, with varying sources and trace element distributions, is needed to determine under which conditions OLS- versus RF models can provide accurate estimates for trace metals.

4.3. Model predictors and interpretation

RF methods provided more interpretable LUR models in most cases, which supports the findings in Ren et al. (2020). RF-LUR models incorporated multiple collinear predictors and drew from a smaller number of variable categories than OLS-LUR models. These results were consistent with the different fundamental principles behind each modelling method. In general, RF-LUR models incorporated predictors from a narrower set of categories and/or subcategories, which makes these models more interpretable. In contrast, OLS-LUR models may have excluded relevant but related source predictors in the same category from constituting the same model, while incorporating combinations of non-collinear proxy predictors from other categories.

Discussions on model predictor comparisons with other PM trace element studies (Brokamp et al., 2017; Chen et al., 2020a, 2020b; De Hoogh et al., 2013; Dirgawati et al., 2016; Ito et al., 2016; Li et al., 2016; Zhang et al., 2015) can be found in section C of the online supplement; as well as other LUR studies that incorporated meteorology (Abernethy et al., 2013; Mavko et al., 2008; Zhang et al., 2015).

4.3.1. Marine transportation and other oil combustion sources

As the busiest port on Canada's east coast, marine vessel emissions and other residual fuel oil combustion sources were expected to contribute significantly to HRM's $PM_{1.0}$. Elements associated with residual fuel oil (RFO) combustion were Ni and V (Agrawal et al., 2008;

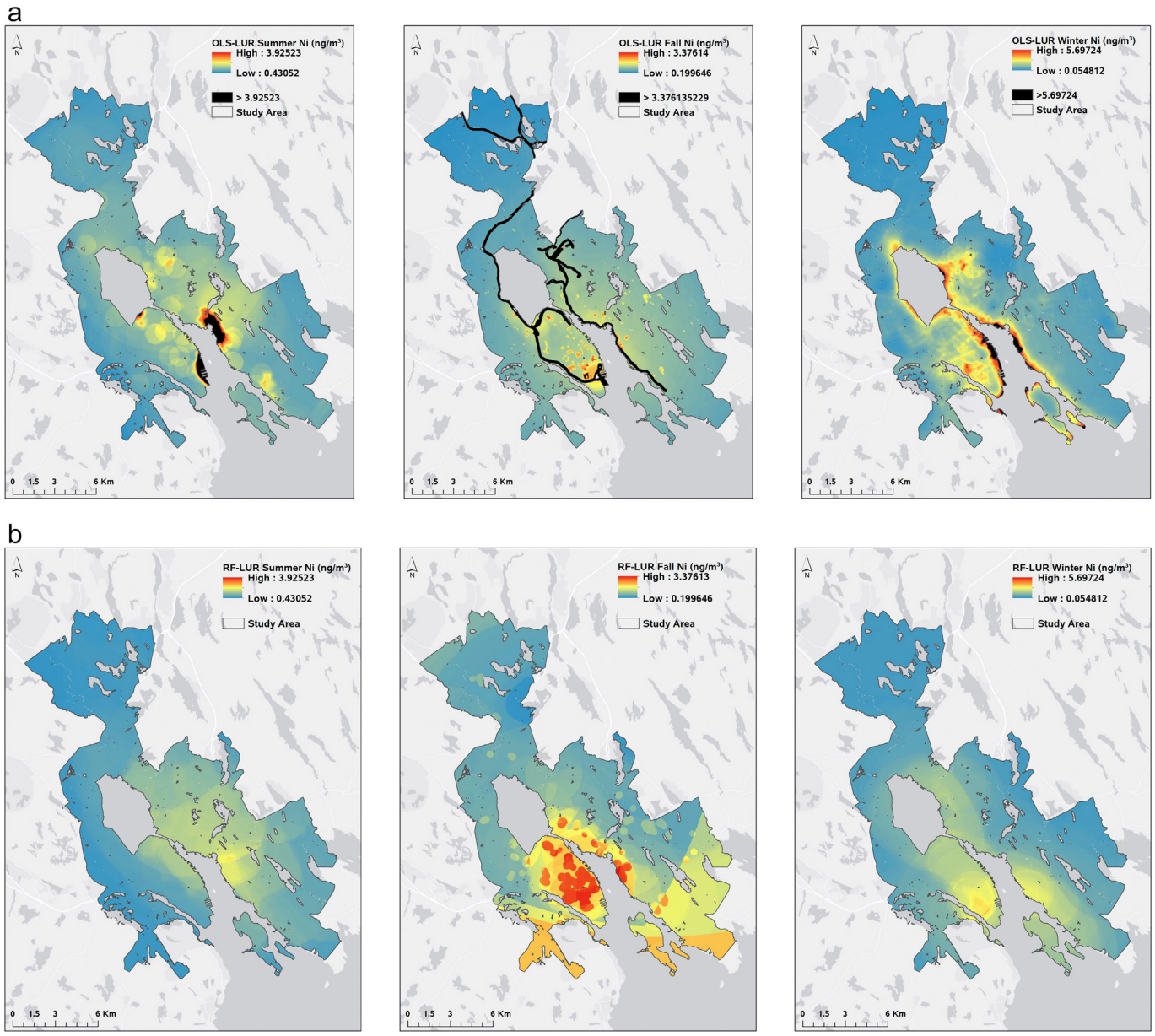

Fig. 4. a: Ni OLS-LUR exposure surfaces in three seasons (left to right: summer, fall, winter). The black areas indicate estimates higher than the maximum measured concentration for that season (not overprediction). Overprediction occurs in the summer and fall surfaces where the maximum predicted concentrations are 199 ng/m^3 and 3.28 × 10^{38} ng/m^3, respectively. b: Ni RF-LUR exposure surfaces in three seasons (left to right: summer, fall, winter). The maximum on the colour scale aligns with the maximum observed concentration for that season.

Celo and Dabek, 2011; Jeong et al., 2011; Lee and Hopke, 2006; Zhao et al., 2013). Ni and V concentrations were highest in winter. Ni spatial variability (CoV) was highest in winter, while V spatial variability was highest in summer. Higher spatial variability in winter is consistent with known inland RFO combustion activities in winter (e.g., institutional heating plants, residential heating, and national military defense facilities).

RF-LUR exposure surfaces for these marker species (Ni shown in Fig. 4) were more readily interpretable compared to OLS-LUR due to the alignment of predictors with known source locations and emission patterns for marine transportation and industrial/institutional oil combustion sources across the seasons. Summer surfaces for Ni, V and S showed higher concentrations near the harbour and downwind of the harbour (i.e., Dartmouth side of HRM by westerly prevailing winds), consistent with ship emissions from vessel traffic in the harbour as well as local point sources with oil combustion emissions (i.e., oil refinery, power generation facility) (Anastasopolos et al., 2021; Environment and Climate Change Canada (ECCC), 2020). For fall and winter, Ni and S RF-LUR maps (winter only for V) differed from the summer as higher concentrations were observed in the more densely developed urban center of HRM. This is consistent with oil combustion used for institutional space heating in this region (i.e., universities, hospitals, and military facilities) and seasonal decrease in ship traffic in colder months (Anastasopolos et al., 2021; Environment and Climate Change Canada (ECCC), 2020).

In general, marine related and industrial variables were important predictors for elements associated with oil combustion (Ni and V). Among the marine related variables, shipyard/ wharf predictors were influential in summer Ni models; while winter models included ocean/coast variables, with a commensurate decrease in contributions from shipyard/wharf predictors. This may reflect near-harbour industrial sources such as power generation (i.e., electricity for residential space heating; (Statistics Canada, 2011)), as well as larger seasonal

contribution from non-marine predictors such as institutional land-use, which may act as indicators of RFO combustion for institutional space heating in winter.

4.3.2. Road and rail transportation sources

Road and railroad transportation predictors had significant contributions to traffic-related $PM_{1.0}$ trace metals (e.g., Ag, Ba, and Cd) in all three seasons. Ba is a meaningful source marker for brake wear-related road and rail traffic emissions (e.g., particles generated by wear of organo-metallic friction brake pads or resuspended from the road or rail surface (Gildemeister et al., 2007; Harrison et al., 2011; Lee and Hopke, 2006)), including in finer size fractions such as $PM_{1.0}$ (Kwak et al., 2013). OLS-LUR generated $PM_{1.0}$-Ba exposure surfaces that were readily interpretable and strongly consistent with the city's transportation network (shown in Fig. 3a). By comparison, the RF-LUR models were less interpretable selecting multiple commercial land use predictors along with some roadway predictors. While commercial predictors were likely suitable proxies for nearby transportation activities, the resulting RF-LUR surfaces did not readily delineate the transportation network where source activity was occurring. Smaller buffer sizes of road predictors may have been selected in winter (versus summer and fall) OLS- and RF-LUR models due to damp conditions reducing Ba dispersion away from the line sources (i.e., reduced brake dust dispersion and resuspension from damp road surfaces and greater PM wash-out by precipitation).

4.3.3. Commercial and industry sources

Commercial variables were strong predictors of $PM_{1.0}$ trace elements in HRM in both OLS- and RF-LUR models, suggesting influences by smaller, spatially distributed localized sources, rather than large single-location industrial facilities. In some cases, these predictors may also be proxies for other sources of trace elements that we were unable to capture. The contribution of commercial variables is equivalent to industrial and institutional/government/military variables combined.

Industrial variables (e.g., facilities reported to NPRI and industrial land-use zoning) were important predictors of airborne trace elements in HRM including for known marker species of oil combustion (Ni and V) as discussed previously in Section 4.3.2.

4.3.4. Biomass combustion sources

The LUR model predictors of intraurban $PM_{1.0}$-K were consistent with biomass combustion source activity (e.g., woodburning for space heating/aesthetics, agricultural woodburning or crop burning, etc.; (Austin et al., 2012; Gibson et al., 2015; Jeong et al., 2011; Masri et al., 2015)) in all three seasons. In the winter OLS-LUR model the top predictor was “fishing & agricultural services”, consistent with woodburning sources (i.e., farms with crop burning, wood burning for space heating, farming waste disposal, fish smoking operations). This predictor was also selected by the RF-LUR model.

Other predictor categories in the fall and winter OLS- and RF-LUR models were smaller roadways, thereby a proxy for residential areas where woodburning is used for supplemental winter space heating in some homes (Statistics Canada, 2011). In the summer OLS- and RF-LUR models, parks/open space land use predictors were selected, consistent with locations of seasonal outdoor or agricultural burning activity.

Both OLS- and RF-LUR methods selected predictors and generated $PM_{1.0}$-K exposure surfaces that were interpretable and consistent with biomass combustion source activity. The RF-LUR model, by virtue of its ability to incorporate collinear predictors, selected a greater range of predictors (e.g., parks/open space in summer models, minor roads in winter) and thus the RF maps may be preferred for this source marker element.

4.4. Seasonal differences

Seasonal differences in predictors may be attributable to differences in seasonal distribution of trace elements' source activity, and meteorology. As discussed in depth in the previous section, seasonal differences in model predictors were consistent with seasonal differences in the distribution of trace elements across the study area, as well as differences in source activity—i.e., household heating, traffic patterns, industrial emissions and outdoor industries (shipping, mining, farming/fishing, etc.).

The inclusion of wind rose predictors in the majority of models suggests that meteorology—particularly the influence of wind direction and speed on air mass trajectories from known upwind source regions—may have played a role in the seasonal differences.

Urban environments have complex land-use where it may be difficult to isolate sources that are co-located or close in proximity. For instance, military facilities (institutional land-use) in HRM includes a naval base located in the port area (marine related). Military facilities also use RFO for winter space heating, thus they report emissions to the NPRI (industrial point source). This could partially explain some of the seasonal differences seen in source predictor categories—where a shift in the seasonal sources may appear as unrelated differences in source categories. In this study, we used national databases without any alternations (i.e., without removing institutions such as military facilities, hospitals and universities from NPRI facilities data).

4.5. Limitations

Low ambient pollutant concentrations posed challenges in modelling some trace elements. Three elements (Cl, Cr, and Hg) were excluded from the study because more than half of the measurements for those elements were below detection in all three seasons. Including elements with only RF-LUR models, eleven elements were modelled in two seasons, and one (Be) was modelled in only one season, due to the high percentage of below DL values in the other seasons. This approach limited seasonal comparisons for some elements. However, we prioritized providing one or two seasonal models over modelling only elements with higher concentrations in all three seasons.

We were unable to conduct external validation (EV) to compare and evaluate model robustness in this study. To our knowledge, this is the first study to measure, characterize and model spatial distribution of $PM_{1.0}$ trace elements in HRM. No previous studies modelling PM trace elements in other cities were able to obtain alternate data to conduct EV, though many commonly modelled criteria pollutants have more data to support EV (Chen et al., 2019). More future studies are needed to characterize and model PM trace elements.

5. Conclusions

We developed 80 seasonal models for $PM_{1.0}$ trace elements in Halifax Regional Municipality—the largest port on Canada's east coast—based on concurrent monitoring at 50 sites across HRM in fall, summer and winter. To our knowledge, this was the first study to compare traditional (OLS) and machine learning (RF) approaches for characterizing the spatial distribution of airborne elements associated with $PM_{1.0}$. Our results demonstrate that RF-LUR were more accurate in most cases; however, in some cases (20–30%) OLS-LUR can be equally or more accurate. This study also identified novel marine industry, transportation, commercial, and meteorological predictors. Our results provide detailed information regarding seasonal and spatial distribution of $PM_{1.0}$ trace elements that will support health studies investigating the long-term impacts of exposure to metals associated with airborne pollutants.

CRediT authorship contribution statement

Joyce J.Y. Zhang: Methodology, Software, Formal analysis, Writing – original draft, Visualization, Validation, Writing – review & editing. **Liu Sun:** Software, Data curation, Visualization, Validation, Formal analysis, Writing – review & editing. **Daniel Rainham:** Conceptualization, Methodology, Investigation, Writing – review & editing. **Trevor J.B. Dummer:** Methodology, Investigation, Writing – review & editing. **Amanda J. Wheeler:** Conceptualization, Methodology, Investigation, Writing – review & editing, Funding acquisition. **Angelos Anastasopolos:** Writing – review & editing. **Mark Gibson:** Investigation, Writing – review & editing. **Markey Johnson:** Conceptualization, Methodology, Software, Writing – original draft, Writing – review & editing, Supervision, Formal analysis, Investigation, Funding acquisition.

Declaration of competing interest

The authors declare that they have no known competing financial interests or personal relationships that could have appeared to influence the work reported in this paper.

Acknowledgments

This study was funded by the Government of Canada's Addressing Air Pollution Horizontal Initiative (AAPHI).

Appendix A. Supplementary data

Supplementary data to this article can be found online at https://doi.org/10.1016/j.scitotenv.2021.150149.

References

Abernethy, R.C., Allen, R.W., McKendry, I.G., Brauer, M., 2013. A land use regression model for ultrafine particles in Vancouver, Canada. Environ. Sci. Technol. 47, 5217–5225.
Agrawal, H., Malloy, Q.G.J., Welch, W.A., Wayne Miller, J., Cocker III, D.R., 2008. In-use gaseous and particulate matter emissions from a modern ocean going container vessel. Atmos. Environ. 42, 5504–5510.
Anastasopolos, A.T., Sofowote, U.M., Hopke, P.K., Rouleau, M., Shin, T., Dheri, A., et al., 2021. Air quality in Canadian port cities after regulation of low-sulphur marine fuel in the North American Emissions Control Area. Sci. Total Environ. 791.
Ault, A.P., Moore, M.J., Furutani, H., Prather, K.A., 2009. Impact of emissions from the Los Angeles port region on San Diego air quality during regional transport events. Environ. Sci. Technol. 43, 3500–3506.
Austin, E., Coull, B., Thomas, D., Koutrakis, P., 2012. A framework for identifying distinct multipollutant profiles in air pollution data. Environ. Int. 45, 112–121.
Bailey, D., Solomon, G., 2004. Pollution prevention at ports: clearing the air. Environ. Impact Assess. Rev. 24, 749–774.
Bertazzon, S., Johnson, M., Eccles, K., Kaplan, G.G., 2015. Accounting for spatial effects in land use regression for urban air pollution modeling. Spatial and Spatio-temporal Epidemiology 14–15, 9–21.
Bivand, R.S., Wong, D.W.S., 2018. Comparing implementations of global and local indicators of spatial association. TEST 27, 716–748.
Brauer, M., Hoek, G., Van Vliet, P., Meliefste, K., Fischer, P., Gehring, U., et al., 2003. Estimating lonq-term average particulate air pollution concentrations: application of traffic indicators and geographic information systems. Epidemiology 14, 228–239.
Breiman, L., 2001. Random forests. Mach. Learn. 45, 5–32.
Brokamp, C., Jandarov, R., Rao, M.B., LeMasters, G., Ryan, P., 2017. Exposure assessment models for elemental components of particulate matter in an urban environment: a comparison of regression and random forest approaches. Atmos. Environ. 151, 1–11.
Cakmak, S., Dales, R., Kauri, L.M., Mahmud, M., Van Ryswyk, K., Vanos, J., et al., 2014. Metal composition of fine particulate air pollution and acute changes in cardiorespiratory physiology. Environ. Pollut. 189, 208–214.
Celo, V., Dabek, E., 2011. In: Anonymous (Ed.), Concentration and Source Origin of Trace Metals in PM2.5 Collected at Selected Canadian Sites Within the Canadian National Air Pollution Surveillance Program, pp. 19–38.
Chen, L., Bai, Z., Kong, S., Han, B., You, Y., Ding, X., et al., 2010. A land use regression for predicting NO2 and PM10 concentrations in different seasons in Tianjin region, China. J. Environ. Sci. 22, 1364–1373.
Chen, J., de Hoogh, K., Gulliver, J., Hoffmann, B., Hertel, O., Ketzel, M., et al., 2019. A comparison of linear regression, regularization, and machine learning algorithms to develop Europe-wide spatial models of fine particles and nitrogen dioxide. Environ. Int. 130.
Chen, J., De Hoogh, K., Gulliver, J., Hoffmann, B., Hertel, O., Ketzel, M., et al., 2020a. Development of Europe-wide models for particle elemental composition using supervised linear regression and random Forest. Environ. Sci. Technol 54, 15698–15709.
Chen, X.-., Cao, J.-., Ward, T.J., Tian, L.-., Ning, Z., Gali, N.K., et al., 2020b. Characteristics and toxicological effects of commuter exposure to black carbon and metal components of fine particles (PM2.5) in Hong Kong. Sci. Total Environ. 742.
Cohen, A.J., Brauer, M., Burnett, R., Anderson, H.R., Frostad, J., Estep, K., et al., 2017. Estimates and 25-year trends of the global burden of disease attributable to ambient air pollution: an analysis of data from the global burden of diseases study 2015. Lancet 389, 1907–1918.
De Hoogh, K., Wang, M., Adam, M., Badaloni, C., Beelen, R., Birk, M., et al., 2013. Development of land use regression models for particle composition in twenty study areas in Europe. Environ. Sci. Technol 47, 5778–5786.
Dirgawati, M., Heyworth, J.S., Wheeler, A.J., McCaul, K.A., Blake, D., Boeyen, J., et al., 2016. Development of land use regression models for particulate matter and associated components in a low air pollutant concentration airshed. Atmos. Environ. 144, 69–78.
DMTI Spatial, 2013. Enhanced Points of Interest.
Environment and Climate Change Canada, 2018. Canadian Environmental Sustainability Indicators: Air Quality.
Environment and Climate Change Canada (ECCC), 2020. National Pollutant Release Inventory (NPRI) 2020.
Environment Canada and Health Canada, 1993. Priority Substances List Assessment Report: Arsenic and Its Compounds.
Environment Canada and Health Canada, 1994a. Priority Substances List Assessment Report: Cadmium and Its Compounds. The Government of Canada.
Environment Canada and Health Canada, 1994b. Priority Substances List Assessment Report: Chromium and Its Compounds.
Environment Canada and Health Canada, 1994c. Priority Substances List Assessment Report: Nickel and Its Compounds.
Environment Canada and Health Canada, 2001. Priority Substances List Assessment Report: Releases From Primary and Secondary Copper Smelters and Copper Refineries - Releases From Primary and Secondary Zinc Smelters and Zinc Refineries.
Enviroware srl, 2016. WindRose PRO.
ESRI. ArcGIS Desktop 2004 and 2012.
European Commission, 2000. Ambient air pollution by As, Cd and Ni compounds. Position Paper.
Microsoft Office Excel 2016.
Fang, T., Guo, H., Zeng, L., Verma, V., Nenes, A., Weber, R.J., 2017. Highly acidic ambient particles, soluble metals, and oxidative potential: a link between sulfate and aerosol toxicity. Environ. Sci. Technol. 51, 2611–2620.
Fishbein, L., 1981. Sources, transport and alterations of metal compounds: an overview. I. Arsenic, beryllium, cadmium, chromium, and nickel. Environ. Health Perspect. 40, 43–64.
Genuer, R., Poggi, J., Tuleau-Malot, C., 2010. Variable selection using random forests. Pattern Recogn. Lett. 31, 2225–2236.
Gibson, M.D., Pierce, J.R., Waugh, D., Kuchta, J.S., Chisholm, L., Duck, T.J., et al., 2013. Identifying the sources driving observed PM2.5 temporal variability over Halifax, Nova Scotia, during BORTAS-B. Atmos. Chem. Phys. 13, 7199–7213.
Gibson, M.D., Haelssig, J., Pierce, J.R., Parrington, M., Franklin, J.E., Hopper, J.T., et al., 2015. A comparison of four receptor models used to quantify the boreal wildfire smoke contribution to surface PM2.5 in Halifax, Nova Scotia during the BORTAS-B experiment. Atmos. Chem. Phys. 15, 815–827.
Gildemeister, A.E., Hopke, P.K., Kim, E., 2007. Sources of fine urban particulate matter in Detroit, MI. Chemosphere 69, 1064–1074.
Government of Canada, 2018. NPRI Data Search.
Harrison, R.M., Beddows, D.C.S., Dall'Osto, M., 2011. PMF analysis of wide-range particle size spectra collected on a major highway. Environ. Sci. Technol 45, 5522–5528.
Health Effects Institute, 2010. Traffic-related Air Pollution: A Critical Review of the Literature on Emissions, Exposure, and Health Effects.
Henderson, S.B., Beckerman, B., Jerrett, M., Brauer, M., 2007. Application of land use regression to estimate long-term concentrations of traffic-related nitrogen oxides and fine particulate matter. Environ. Sci. Technol. 41, 2422–2428.
Hoek, G., Beelen, R., de Hoogh, K., Vienneau, D., Gulliver, J., Fischer, P., et al., 2008. A review of land-use regression models to assess spatial variation of outdoor air pollution. Atmos. Environ. 42, 7561–7578.
Hoek, G., Krishnan, R.M., Beelen, R., Peters, A., Ostro, B., Brunekreef, B., et al., 2013. Long-term air pollution exposure and cardio-respiratory mortality: a review. Environ. Health Glob. Access Sci. Sour. 12.
Hsu, C., Wu, C., Hsiao, Y., Chen, Y., Chen, M., Lung, S.-C., 2018. Developing land-use regression models to estimate PM 2.5 -bound compound concentrations. Remote Sens. 10.
Ito, K., Johnson, S., Kheirbek, I., Clougherty, J., Pezeshki, G., Ross, Z., et al., 2016. Intraurban variation of fine particle elemental concentrations in New York City. Environ. Sci. Technol. 50, 7517–7526.
Jeong, C.-., McGuire, M.L., Herod, D., Dann, T., Dabek-Zlotorzynska, E., Wang, D., et al., 2011. Receptor model based identification of PM2.5 sources in Canadian cities. Atmos. Pollut. Res. 2, 158–171.
Jerrett, M., Arain, M.A., Kanaroglou, P., Beckerman, B., Crouse, D., Gilbert, N.L., et al., 2007. Modeling the intraurban variability of ambient traffic pollution in Toronto, Canada. J. Toxic. Environ. Health A 70, 200–212.
Kanaroglou, P.S., Jerrett, M., Morrison, J., Beckerman, B., Arain, M.A., Gilbert, N.L., et al., 2005. Establishing an air pollution monitoring network for intra-urban population exposure assessment: a location-allocation approach. Atmos. Environ. 39, 2399–2409.
Kerckhoffs, J., Hoek, G., Gehring, U., Vermeulen, R., 2021. Modelling nationwide spatial variation of ultrafine particles based on mobile monitoring. Environ. Int. 154.
Kuwayama, T., Ruehl, C.R., Kleeman, M.J., 2013. Daily trends and source apportionment of ultrafine particulate mass (PM0.1) over an annual cycle in a typical California city. Environ. Sci. Technol. 47, 13957–13966.

Kwak, J.-., Kim, H., Lee, J., Lee, S., 2013. Characterization of non-exhaust coarse and fine particles from on-road driving and laboratory measurements. Sci. Total Environ. 458–460, 273–282.
Lack, D.A., Cappa, C.D., Langridge, J., Bahreini, R., Buffaloe, G., Brock, C., et al., 2011. Impact of fuel quality regulation and speed reductions on shipping emissions: implications for climate and air quality. Environ. Sci. Technol. 45, 9052–9060.
Lee, J.H., Hopke, P.K., 2006. Apportioning sources of PM2.5 in st. Louis, MO using speciation trends network data. Atmos. Environ. 40, 360–377.
Li, H.Z., Dallmann, T.R., Gu, P., Presto, A.A., 2016. Application of mobile sampling to investigate spatial variation in fine particle composition. Atmos. Environ. 142, 71–82.
Liaw, A., Wiener, M., 2001. Classification and regression by RandomForest. Forest 23.
Liu, Y., Goudreau, S., Oiamo, T., Rainham, D., Hatzopoulou, M., Chen, H., et al., 2020. Comparison of land use regression and random forests models on estimating noise levels in five Canadian cities. Environ. Pollut. 256.
Lockeretz, W., 1974. Deposition of airborne mercury near point sources. Water Air Soil Pollut. 3, 179–193.
Madsen, C., Gehring, U., Håberg, S.E., Nafstad, P., Meliefste, K., Nystad, W., et al., 2011. Comparison of land-use regression models for predicting spatial NOx contrasts over a three year period in Oslo, Norway. Atmos. Environ. 45, 3576–3583.
Masiol, M., Squizzato, S., Formenton, G., Khan, M.B., Hopke, P.K., Nenes, A., et al., 2020. Hybrid multiple-site mass closure and source apportionment of PM2.5 and aerosol acidity at major cities in the Po Valley. Sci. Total Environ. 704.
Masri, S., Kang, C.-., Koutrakis, P., 2015. Composition and sources of fine and coarse particles collected during 2002–2010 in Boston, MA. J. Air Waste Manag. Assoc. 65, 287–297.
Mavko, M.E., Tang, B., George, L.A., 2008. A sub-neighborhood scale land use regression model for predicting NO2. Sci. Total Environ. 398, 68–75.
Millward, H., Spinney, J., 2011. Time use, travel behavior, and the rural-urban continuum: results from the Halifax STAR project. J. Transp. Geogr. 19, 51–58.
Mukerjee, S., Smith, L.A., Johnson, M.M., Neas, L.M., Stallings, C.A., 2009. Spatial analysis and land use regression of VOCs and NO2 from school-based urban air monitoring in Detroit/Dearborn, USA. Sci. Total Environ. 407, 4642–4651.
Ostro, B., Hu, J., Goldberg, D., Reynolds, P., Hertz, A., Bernstein, L., et al., 2015. Associations of mortality with long-term exposures to fine and ultrafine particles, species and sources: results from the California teachers study cohort. Environ. Health Perspect. 123, 549–556.
Paradis, E., Ape, Schliep K., 2019. 5.0: an environment for modern phylogenetics and evolutionary analyses in R. Bioinformatics 35, 526–528.
Perez, L., Künzli, N., Avol, E., Hricko, A.M., Lurmann, F., Nicholas, E., et al., 2009. Global goods movement and the local burden of childhood asthma in southern California. Am. J. Public Health 99 (Suppl. 3), S622–S628.
Raaschou-Nielsen, O., Andersen, Z.J., Beelen, R., Samoli, E., Stafoggia, M., Weinmayr, G., et al., 2013. Air pollution and lung cancer incidence in 17 European cohorts: prospective analyses from the European study of cohorts for air pollution effects (ESCAPE). Lancet Oncol. 14, 813–822.
Reid, C.E., Jerrett, M., Petersen, M.L., Pfister, G.G., Morefield, P.E., Tager, I.B., et al., 2015. Spatiotemporal prediction of fine particulate matter during the 2008 northern California wildfires using machine learning. Environ. Sci. Technol. 49, 3887–3896.
Ren, X., Mi, Z., Georgopoulos, P.G., 2020. Comparison of machine learning and land use regression for fine scale spatiotemporal estimation of ambient air pollution: modeling ozone concentrations across the contiguous United States. Environ. Int. 142.
Requia, W.J., Coull, B.A., Koutrakis, P., 2019. Evaluation of predictive capabilities of ordinary geostatistical interpolation, hybrid interpolation, and machine learning methods for estimating PM2.5 constituents over space. Environ. Res. 175, 421–433.
Rivera, M., Basagaña, X., Aguilera, I., Agis, D., Bouso, L., Foraster, M., et al., 2012. Spatial distribution of ultrafine particles in urban settings: a land use regression model. Atmos. Environ. 54, 657–666.
R-Project, 2017. R.
Ryan, P.H., Lemasters, G.K., 2007. A review of land-use regression models for characterizing intraurban air pollution exposure. Inhal. Toxicol. 19, 127–133.
SAS, 2008. SAS Institute.
SAS, 2013. SAS Institute.
Song, X.-., Polissar, A.V., Hopke, P.K., 2001. Sources of fine particle composition in the northeastern US. Atmos. Environ. 35, 5277–5286.
Statistics Canada, 2008. Canada Census Digital Boundary File/Digital Cartographic File 2006.
Statistics Canada, 2011. Households and the Environment: Energy Use Catalogue no. 11-526-S.
Statistics Canada, 2012. Focus on Geography Series, 2011 Census. Statistics Canada Catalogue no. 98-310-XWE2011004.
Statistics Canada, 2017. Households and the Environment Survey: Household Characteristics, 2015.
Su, J.G., Jerrett, M., Beckerman, B., Verma, D., Arain, M.A., Kanaroglou, P., et al., 2010. A land use regression model for predicting ambient volatile organic compound concentrations in Toronto, Canada. Atmos. Environ. 44, 3529–3537.
Tian, L., Ho, K.-., Louie, P.K.K., Qiu, H., Pun, V.C., Kan, H., et al., 2013. Shipping emissions associated with increased cardiovascular hospitalizations. Atmos. Environ. 74, 320–325.
Tripathy, S., Tunno, B.J., Michanowicz, D.R., Kinnee, E., Shmool, J.L.C., Gillooly, S., et al., 2019. Hybrid land use regression modeling for estimating spatio-temporal exposures to PM 2.5, BC, and metal components across a metropolitan area of complex terrain and industrial sources. Sci. Total Environ. 673, 54–63.
Vienneau, D., de Hoogh, K., Beelen, R., Fischer, P., Hoek, G., Briggs, D., 2010. Comparison of land-use regression models between Great Britain and the Netherlands. Atmos. Environ. 44, 688–696.
Weichenthal, S., Ryswyk, K.V., Goldstein, A., Bagg, S., Shekkarizfard, M., Hatzopoulou, M., 2016. A land use regression model for ambient ultrafine particles in Montreal, Canada: a comparison of linear regression and a machine learning approach. Environ. Res. 146, 65–72.
Wheeler, A.J., Smith-Doiron, M., Xu, X., Gilbert, N.L., Brook, J.R., 2008. Intra-urban variability of air pollution in Windsor, Ontario-measurement and modeling for human exposure assessment. Environ. Res. 106, 7–16.
Zhang, J.J.Y., Sun, L., Barrett, O., Bertazzon, S., Underwood, F.E., Johnson, M., 2015. Development of land-use regression models for metals associated with airborne particulate matter in a North American city. Atmos. Environ. 106, 165–177.
Zhao, M., Zhang, Y., Ma, W., Fu, Q., Yang, X., Li, C., et al., 2013. Characteristics and ship traffic source identification of air pollutants in China's largest port. Atmos. Environ. 64, 277–286.